J. Mol. Biol. (1998) **278**, 389–400

JMB

Nucleotide-dependent Structural Changes in Dimeric NCD Molecules Complexed to Microtubules

K. Hirose[1], R. A. Cross[2] and L. A. Amos[3]*

[1]*National Institute for Advanced Interdisciplinary Research, Tsukuba 305, Japan*

[2]*Marie Curie Research Institute, Oxted, UK*

[3]*MRC Laboratory of Molecular Biology, Hills Road, Cambridge CB2 2QH, UK*

**Corresponding author*

Complexes consisting of motor domains of the kinesin-like protein ncd bound to reassembled brain microtubules were visualised using cryoelectron microscopy and helical image reconstruction. Different nucleotide-associated states of a dimeric construct (NΔ295-700) of ncd were analysed to reveal ADP-containing, AMP.PNP-containing and empty (rigor) conformations. In these three states, each thought to mimic a different stage in ATP turnover, the double-headed motors attach to the microtubules by one head only, with the free head tethered in relatively fixed positions. The three structures differ both in the way the attached heads interact with tubulin and in the position of the tethered heads. In the strongly binding rigor and AMP.PNP (ATP-like) states, the attached head makes close contact with both subunits of a tubulin heterodimer. In the weakly bound ADP state, the contact made by the attached head with the monomer closer to the plus end appears to be more loose. Also, in the ATP-like state, the free head tilts nearer to the plus end than in the other two states. The data argue against model mechanisms in which a conformational change in the bound head guides the free head closer to its next binding site; on the contrary, the transition from ADP-filled *via* rigor to the AMP.PNP (ATP-like) state of the bound head produces a small motion of the free head in the counter-productive direction. However, the observation that the tethered head points towards the minus end, in all three states, is consistent with the idea that the relative arrangement of the heads in a dimer is a major determinant of directionality.

Keywords: kinesin-like; molecular motor; cryoelectron microscopy; 3-D image reconstruction; cell motility

Introduction

Ncd (non claret disjunctional) is a kinesin-related motor molecule involved in the formation of meiotic and mitotic spindles in *Drosophila* (Sawin & Endow, 1993). In contrast with kinesin itself, which moves towards the faster-growing or ''plus'' end of microtubules (Vale *et al*., 1985), ncd moves along microtubules toward the minus end (Macdonald *et al*., 1990; Walker *et al*., 1990). Also, whereas the ~340 amino acid ATPase-domain or ''head'' of kinesin lies at the N terminus of the polypeptide (Yang *et al*., 1989), the highly homologous head of ncd is at its C terminus (Macdonald *et al*., 1990). In both molecules, the α-helical stalk domain, to which the head is attached, dimerises to form a coiled-coil (de Cuevas *et al*., 1992; Morii *et al*., 1997; Song & Mandelkow, 1994; Tripet *et al*., 1997)). When truncated proteins are expressed *in vitro*, kinesin constructs of more than ~380 amino acids dimerise (Gelles *et al*., 1995; Huang *et al*., 1994; Jiang *et al*., 1997; Moyer *et al*., 1996). Ncd constructs that start before residue 300 also dimerise (Chandra *et al*., 1993).

The conformational mechanisms by which kinesin and ncd make mutually opposite progress along microtubules are largely unknown. Clearly, the turnover of nucleotide in the motor active sites drives conformational changes, which in turn drive the motors along the microtubules, but the nature of these conformational changes is mysterious. The kinetic mechanisms (the chemical mechanism of ATP turnover) appear similar (Lockhart & Cross, 1994; Amos & Cross, 1997) but it is possible that the mechanism of coupling of the active site chem-

Abbreviations used: 3-D, three-dimensional; pf, protofilament; ncd, non-claret disjunctional protein from *Drosophila*.

0022–2836/98/170389–12 $25.00/0/mb981709

istry to directional progress is different. Specifically, the two motors may differ in their processivity: there is very good evidence that two-headed kinesin takes runs of 100 or more steps along microtubules (Jiang & Hackney, 1997). Two-headed ncd does not seem to do this (Case *et al*., 1997; Crevel *et al*., 1997), though the possibility remains it may make short bursts of steps before detaching. Analysis of kinesin sequence immediately following the catalytic domain indicates that much of it has the potential to form a coiled coil; but a set of destabilising insertions may induce it to unzip, perhaps transiently, allowing the motor domains intermittently to splay apart and bridge between adjacent binding sites on the microtubule (Hackney, 1994; Tripet *et al*., 1997). In contrast, the stretch of sequence at the N terminus of ncd's catalytic domain is predicted to form unbroken coiled coil (Crevel *et al*., 1997), which would be consistent with ncd's apparent lack of processivity.

The role of the dimerisation domain in constraining and determining the stepping action of the motor is more profound than initially thought. Earlier, work on kinesin and ncd constructs with spectrin or GST tails had indicated that the properties determining the direction of movement of a kinesin-like protein lay solely in the motor domain (Stewart *et al*., 1993). Recently, however, Henningsen & Schliwa (1997) and Case *et al*. (1997) have shown that ncd-kinesin chimaeras, consisting of the ncd motor domain attached by its C terminus to a kinesin ''neck'' and stalk, move towards the plus end of microtubules. This proves that the direction of movement is not ultimately determined by any directional behaviour of the motor domain; at least in the case of dimeric ncd, the position of the motor domains relative to the tail or the properties of the neck are more important factors. The failure of Stewart *et al*. (1993) to reverse the direction of kinesin by attaching a tail to its N terminus is thought to be due to retention of a small section of the kinesin neck at the C terminus (Case *et al*., 1997).

An obvious approach to understanding the mechanism is to attempt to visualise the mechanical action of the motor directly. Three-dimensional (3-D) maps of microtubules complexed with dimeric motor domains in the presence of AMP-PNP have previously been obtained from cryo-electron microscope images (Arnal *et al*., 1996; Hirose *et al*., 1996) and show the motors attached to tubulin by one of their two heads. The tethered head of kinesin lies closer to the microtubule plus end but the tethered head of ncd points towards the minus end. These results suggested that the orientations of the head domains might be important in determining the opposite directions of movement along microtubules of these otherwise very similar motors.

In the work reported here, we have used cryo-electron microscopy and 3-D image analysis to visualise complexes of a dimeric construct of ncd (NΔ295-700), attached to reassembled brain microtubules, in three states thought to mimic different stages in ATP turnover (Amos & Cross, 1997): the strong binding rigor (no nucleotide) and AMP.PNP (ATP-like) states, and the weak binding ADP state. All three conformational states are different. The movements we see allow us to rule out models in which the tilting of a ''lever arm'' within the bound head guides the free head closer to its next binding site.

Results

Microtubules reassembled from purified brain tubulin were used, following the observation by Sosa & Milligan (1996) that many of the 15-protofilament microtubules included in such samples have full helical symmetry. Microtubules mixed with motor molecules in the presence of AMP.PNP or absence of nucleotide (see Materials and Methods) all appeared to be fully decorated after being frozen for cryoelectron microscopy (Figure 1). However, the extent to which microtubules were decorated with motor molecules in the ADP-filled state was greatly affected by minor variations in the freezing conditions. Hence the experiments with ADP present were repeated many more times than for the tightly binding states. Although the microtubules looked fully decorated in the pre-

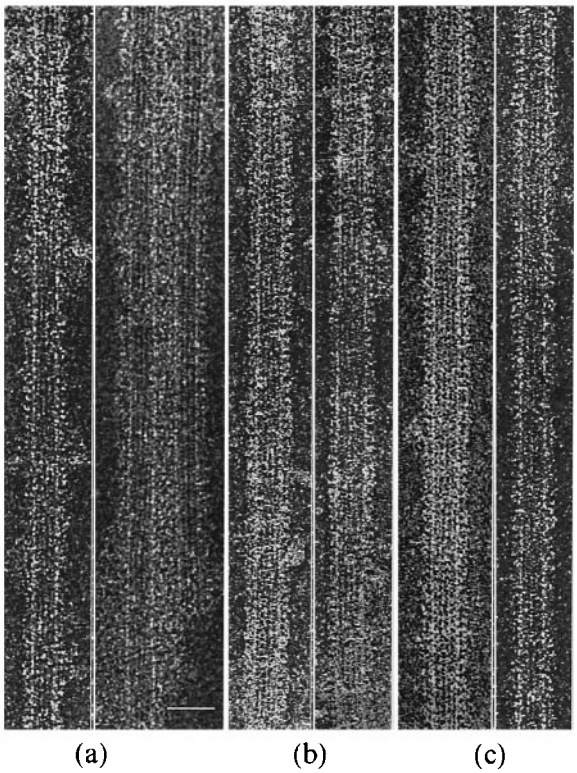

Figure 1. Electron microscope images of brain microtubules decorated with the double-headed ncd motor construct (NΔ295-700): (a) in the presence of ADP and hexokinase; (b) in the absence of free nucleotide, with apyrase; (c) in the presence of AMP.PNP and apyrase. Scalebar represents 50 nm.

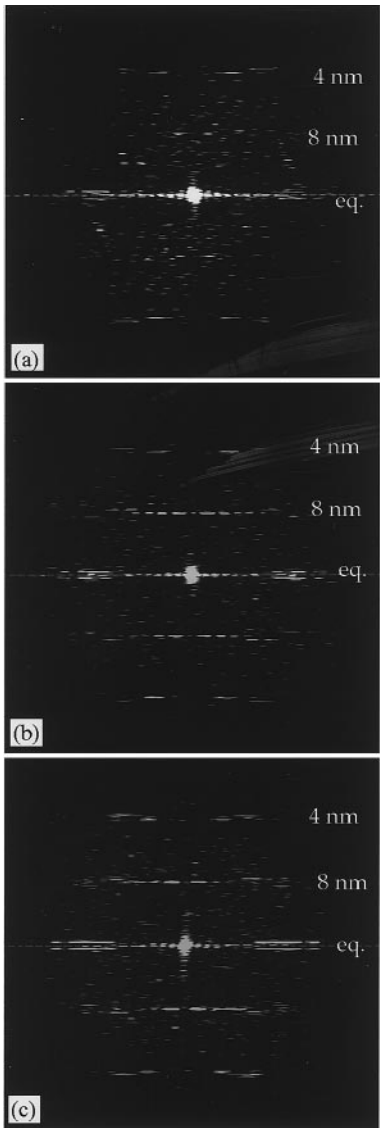

Figure 2. Computed diffraction patterns from images such as those in Figure 1. The equatorial (eq.) and 8 nm layerlines are relatively weaker in a pattern from an ADP-containing complex (a) than for nucleotide-free (b) or AMP.PNP-associated specimens (c).

sence of ADP, the 8 nm layerline in their diffraction patterns were weaker than in patterns from the other two states (Figure 2). Most of the images selected by measuring their diameters were determined during computer analysis to be of 15-protofilament (15-pf) microtubules, apart from two good 16-protofilament (16-pf) specimens found among the ADP-containing complexes.

Each digitised image was analysed by calculating its Fourier transform and plotting the amplitudes and phases along each half-layerline (see Figure 3(a)). Amongst thousands of images of complexes in ADP, 11 images of 15-protofilament microtubules showed clear evidence of helical symmetry. The analysis of complexes in AMP.PNP and no nucleotide was continued until eight good images of helical 15-protofilament tubules were found in each category. Diffraction patterns from all of these images included the near-equatorial (15,0) layerline, two of those in the 8 nm group of layerlines ((−2,1) and (13,1)) and two in the 4 nm group ((−4,2) and (11,2)) (Figure 3). The weaker (−17,1) and (−19,2) layerlines could also be seen in many. Some patterns also had (−6,3) and (−8,4) layerline peaks, taking the resolution to 2 nm but these data, being relatively weak, were not included in the present analysis.

Figure 3(a) compares the amplitudes and phases in a selection of individual half transforms. The amplitude peaks on layerlines derived from different images of the same type show quite large variations; this is probably partly due to sampling error, since the averaged values along most layerlines are comparable for different states (see Figure 3(b)). The relative weakness of the 8 nm layerline for the ADP-containing state (Figure 2(a) and (−2,1) in Figure 3) is, therefore, significant. A weak 8-nm layerline could be due to disordering of the ncd molecules in this state, if weakly attached motors are more free to vary their orientations. A possible alternative reason is that a significant number of binding sites on the microtubules might not be occupied.

In general, the phase values from different images agree quite closely where the amplitudes are strong but show large variations between the amplitude peaks (Figure 3(a)). However, some datasets included layerlines on which the phases were clearly different from the general consensus, for example on the (11,2) layerline. It is difficult to explain such deviations in terms of random noise; possibly these specimens were distorted in some way. Such datasets were omitted from the average values used to calculate the final maps (see later). However, all the datasets (22 ''near-sides'' plus ''far-sides'' for ADP-containing complexes, 16 for each of the other two states) contributed to the results in helping to define the consensus phases for each type of specimen and the statistical differences described next.

The averaged datasets for different classes of specimens were cross-correlated in the same manner as individual datasets were compared within their own class. The phase values plotted in Figure 3 thus correspond to relative orientations that gave the best overall fit between different types of specimen. The averaged datasets (Figure 3(b)) are clearly quite similar but there are statistically significant differences in both amplitudes and phases. Although the averaged amplitudes for different states tend to be very comparable, there are, for example, differences on the 8 nm/(−2,1) layerline for weakly bound *versus* strongly bound states. The 13-fold function on the 8-nm group of layerlines ((13,1) in Figure 3(b)) differs in amplitude values, and also in phase by more than the corresponding standard deviations among the three types of specimen. The centre of the main peak for AMP.PNP (arrow) occurs at a

radial spacing where the other specimens have minima and the phase value there differs by around 180°. Plots in Figure 3(c) for (14,1) , the equivalent layerline for 16-pf microtubules, show similar differences for AMP.PNP as compared with ADP.

The most significant feature of the ADP data, compared with the other two states, is associated with the near-equatorial layerline, which arises from the protofilament spacing (i.e. (15,0) in Figure 3(b)). Although the second peak (dominated by contributions from tubulin) has a similar phase distribution for all three averages, the first peak has different phases (indicated by arrows). There is a corresponding difference for the (16,0) layerline

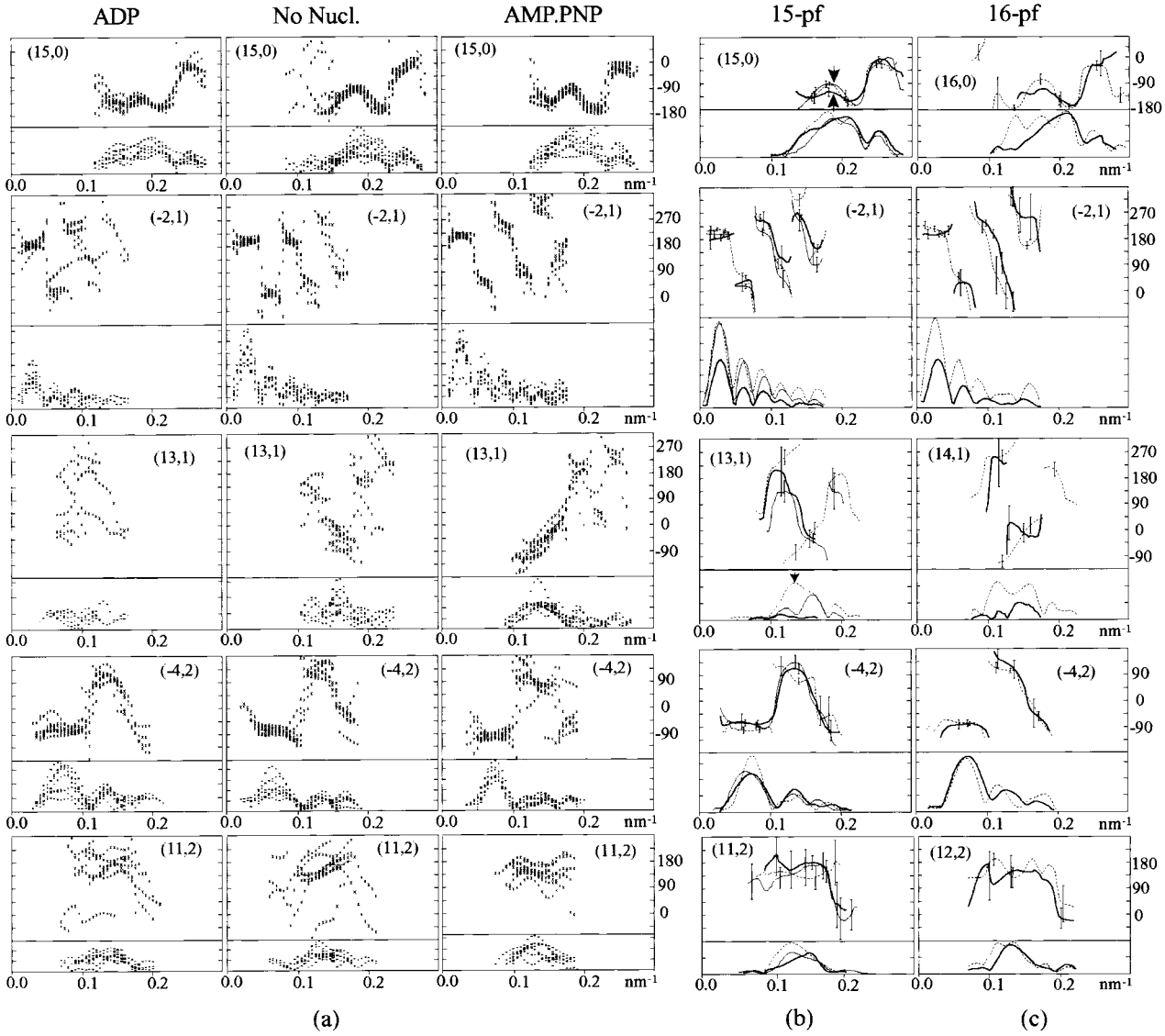

Figure 3. (a) Distributions of phases and amplitudes along the main layerlines in Fourier transforms, computed from individual images of decorated 15-protofilament brain microtubules. Phases (in degrees) are shown in the upper plot of each panel, amplitudes (all on the same scale) in the lower plots. The phases for each individual image have been corrected for a rotation about the microtubule axis and for a shift in the position of the phase origin along the axis; these values being chosen to give the best overall agreement between different images. The layerline indexing (*n*,*l*) refers to the Bessel order *n*, or number of equivalent helices, and the layerline number *l*, based on a nominal 8 nm axial repeat. The plots are labelled to show whether the data are from specimens decorated in the presence of ADP or AMP.PNP, or in the absence of nucleotides. (b), (c) Comparison of averaged amplitudes and phases. (b) Data for the three sets of images of decorated 15-protofilament brain microtubules (thicker lines, ADP data; thinner continuous lines, no nucleotide data; broken lines, AMP.PNP data). In (c) data for images of 16-pf brain tubules decorated in the presence of ADP (thicker lines) are compared with those of 16-pf cricket tubules decorated in the presence of AMP.PNP (broken lines). Standard deviations are shown on the phase plots at various radii where there are peaks in amplitude. All amplitudes are shown on the same scale. The effect of AMP.PNP, compared with the other two states, is most clearly seen on the (13,1) layerline (arrowhead). The effect of ADP is most obvious as a difference in the phases along the first peak on the (15,0) layerline (arrows); the corresponding difference in real space is shown in Figure 4.

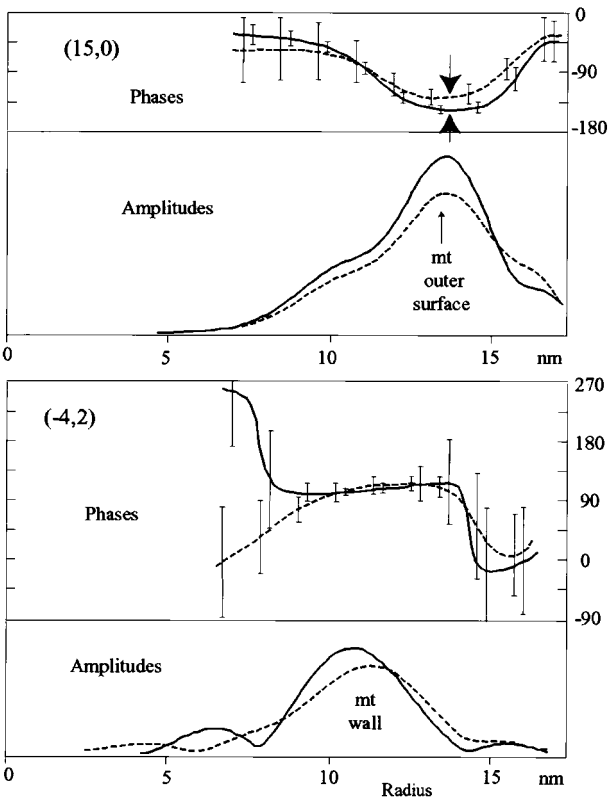

Figure 4. Some of the real-space functions ($g_{n,l}(r)$) for ADP-containing (continuous line) and nucleotide-free specimens (broken line), calculated from average reciprocal space functions shown in Figure 3(b). The (−4,2) functions, which produce density variations with a 4 nm axial repeat in the 3-D maps, mainly affect the density distribution in the microtubule; phase values for the two states differ only where the amplitudes are weak. In contrast, the (15,0) functions, which produce the ~5 nm longitudinal protofilament spacing, show a small but significant phase difference at the amplitude peak; at the radial distance indicated by arrows, where the motor domains are attached to the microtubule, the standard deviations in the phase values do not overlap.

in Figure 3(c). The effect of these differences in the reciprocal space functions ($G_{n,l}(R)$), when transformed into the real-space functions ($g_{n,l}(r)$) is shown in Figure 4. The (15,0) functions for ADP-containing and nucleotide-free specimens have a significant phase difference at a radius corresponding to the outside surface of the microtubule; the effect of this difference on the 8 nm-spaced ncd molecules in the reconstructed images (see blue arrows in Figure 5) is described below. In contrast, the microtubule-dominated (−4,2) functions differ in phase only where the amplitudes are very weak.

Maps calculated for decorated 15-protofilament tubules in the three nucleotide states are shown in Figure 5. The averaged data included only individual datasets for which all of the main layerlines conformed to the consensus, since the inclusion of non-conforming data had the effect of smearing the positions of the ncd motor domains and thereby weakening their densities. When the density of the motor domains relative to the microtubule is weak, it becomes difficult to represent the structure by means of a single contour level, as required for the surface representations. Including all of the datasets does not change the positions of the main features, however.

In each map, the tubulin protofilaments (coloured green) appear very similar to those in earlier maps (Hirose *et al.*, 1996, 1997). The sites to which the attached heads (coloured yellow) are bound are basically unchanged by the nucleotide state. As expected from the differences in the layerline data, the three maps reveal small conformational changes in the ncd molecules. The most obvious change is in the position of the tethered head (coloured orange), relative to the attached head. Compared with the structure in the presence of ADP or no nucleotide, in AMP.PNP the tethered heads are closer to the plus end of the microtubule by about 0.3 nm. Cross-sections (Figure 6) and sections along the axis (Figure 7) confirm that the position of the tethered head (H2 in Figure 7, asterisks in Figure 6) changes relative to the tubulin subunits, whilst that of the attached head (H1) stays constant.

The effect of ADP relative to no nucleotide is more subtle. Both heads have reduced density in maps of the ADP-containing state (see Figures 6 and 7) though they appear to be centred on approximately the same positions as in the absence of nucleotide. Difference maps (not shown) between the ADP-filled and empty structures are dominated by changes in the overall density in the motor domains. Therefore, changes in the positions and shapes of the attached heads due to ADP are difficult to pin-point. However, the change in the phases on the (15,0) layerline (Figures 3(b) and 4) indicates that their average position is slightly different from that of strongly attached heads. In particular, although the nucleotide-free motor domain appears to interact equally with two tubulin monomers, the ADP-filled motor tilts slightly so that it interacts more weakly (as indicated by arrows in Figures 5(d) and 7(a) and (e)) with the subunit closer to the microtubule plus end, that is, the beta-tubulin monomer (reviewed by Amos & Hirose, 1997). As shown later, this change in connectivity is a consequence of the phase difference on the (15,0) layerline (Figures 3(b) and 4). There also appear to be subtle changes in the shapes of the heads that may be significant (see Discussion and Figures 5 and 9).

The map derived from 16-pf brain microtubules decorated in the presence of ADP, being derived from a very small population of images, is noisier than that from the 15-pf microtubules. The noise affects the surface representation most badly (Figure 9(a)(ii)). The main features are better represented by the contour maps (Figures 6 and 7), where features described for the 15-pf complex in ADP are also present in the 16-pf complex.

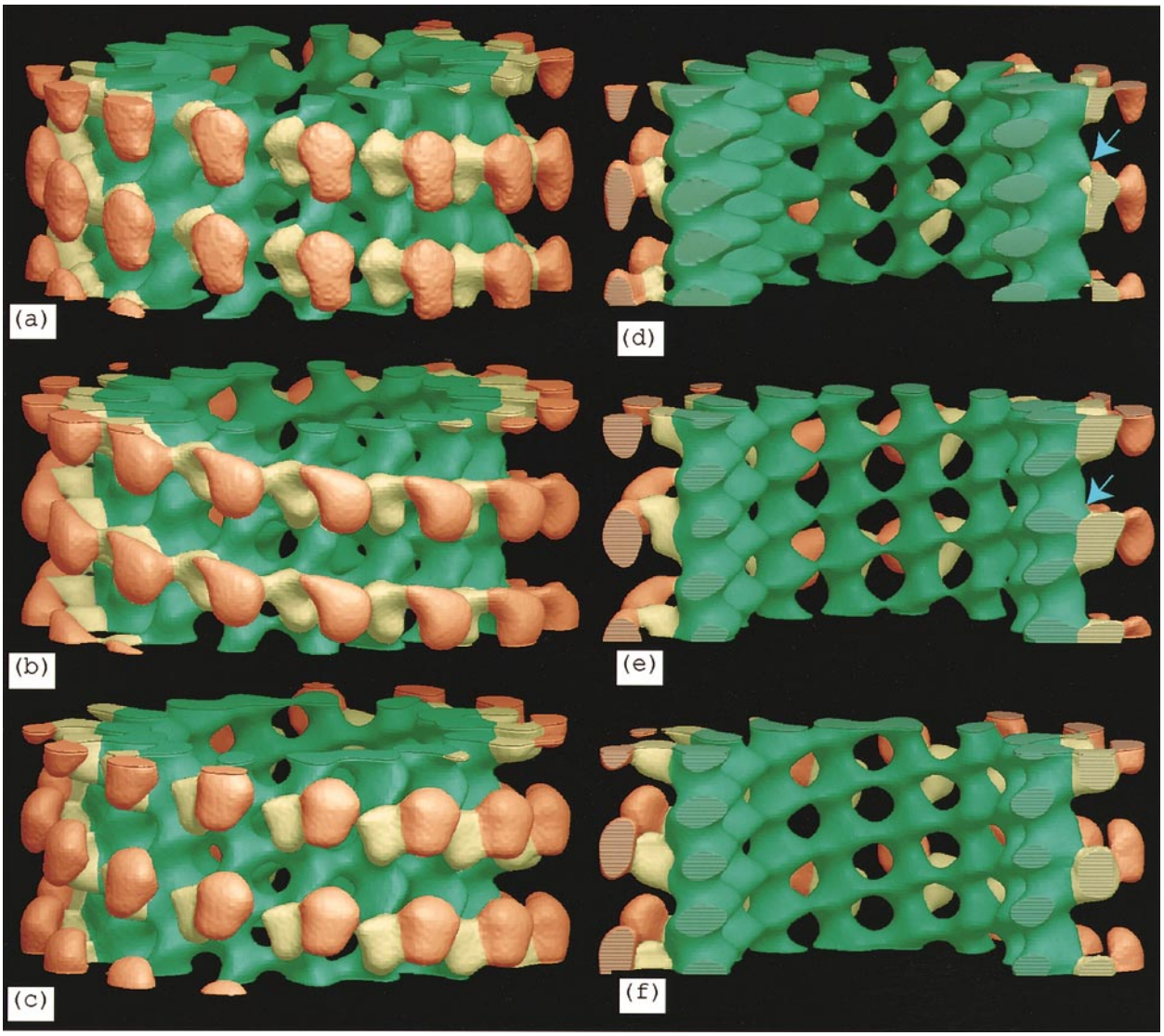

Figure 5. Surface representations of 3-D density maps computed from averaged data for 15-protofilament brain microtubules decorated with dimeric ncd. (a) and (d) show the complex formed in the presence of ADP (average of eight datasets from five images), (b) and (e) that in the absence of free nucleotide (average of eight datasets from six images) and (c) and (f) that in the presence of AMP.PNP (average of eight datasets from four images). Each map is oriented with the microtubule plus end at the top of the page. Tubulin has been coloured green, bound heads are yellow and second heads, not attached directly to tubulin, are orange. (d) to (f) Have been sectioned so as to show the inside surfaces; there are no obvious changes in tubulin due to conformational changes in the attached motor domains. A higher contour level than that in (a) to (c) has been chosen in order to show details of the interaction between tubulin and ncd (indicated by blue arrows), which is weakened in the ADP-containing complex.

It was important to check that the difference found between the nucleotide-free and ADP-containing states does not merely reflect the weakness of the 8 nm layerline, which might simply be due to a lack of decoration. The Fourier amplitudes in the two states were therefore averaged in order to calculate a pair of more comparable maps. Figure 8(a) and (c) shows sections through two hybrid maps calculated using the same amplitude values but with independent sets of phases; for Figure 8(a) the averaged amplitudes were combined with the phases from the ADP state, for Figure 8(c) they were combined with the phases from the nucleotide-free state. The two maps have the same features as the fully independent maps in Figure 7(a) and (b), indicating that the most important distinction between these two states lies in the phase information. Finally, Figure 8(b) shows that the ADP-containing structure can be made more like the nucleotide-containing structure by changing only the phases on the (15,0) layerline. The phase shift, though small, is significant, being larger than the standard deviations in the corresponding region of the layerline (Figure 3(b)), so we conclude that the structural difference

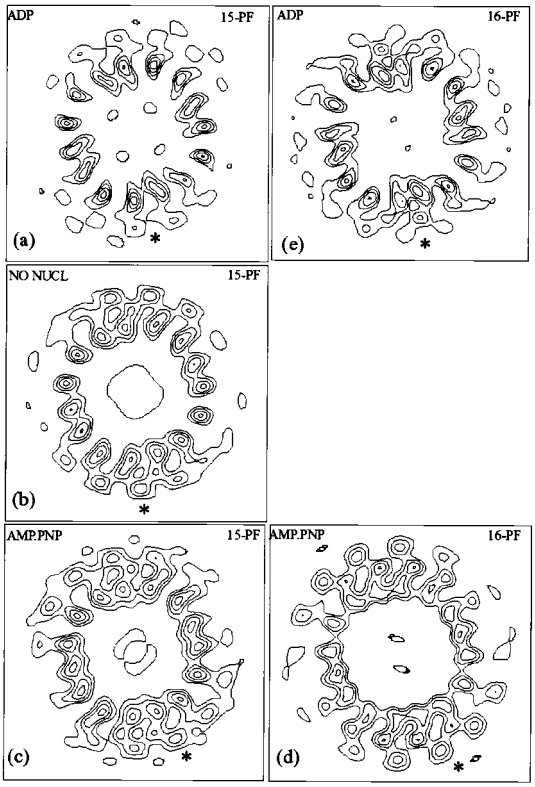

Figure 6. Cross-sections through each of the five independent maps calculated from the data in Figure 3(b) and (c). (a) to (c) Are sections through the maps shown in Figure 5, as viewed from the microtubule plus end; (d) is a section through the map of 16-pf microtubules decorated in the presence of ADP (average of four datasets), as shown in Figure 9(a)/(ii); (e) is a section through a map of 16-pf cricket microtubules decorated in AMP.PNP (five datasets, now averaged in reciprocal space, as opposed to the almost identical real-space-averaged map published by Hirose *et al.* (1996)), shown also in Figure 9(a)/(viii). In each section, adjacent protofilaments are cut at different levels; thus successive protofilaments in a clockwise direction show sections closer to the minus end of the microtubule. The three maps of 15-protofilament microtubules are oriented to put tubulin dimers and attached ncd heads in equal positions. Asterisks mark the centres of the outer heads; they are further anticlockwise in the maps of specimens containing AMP.PNP.

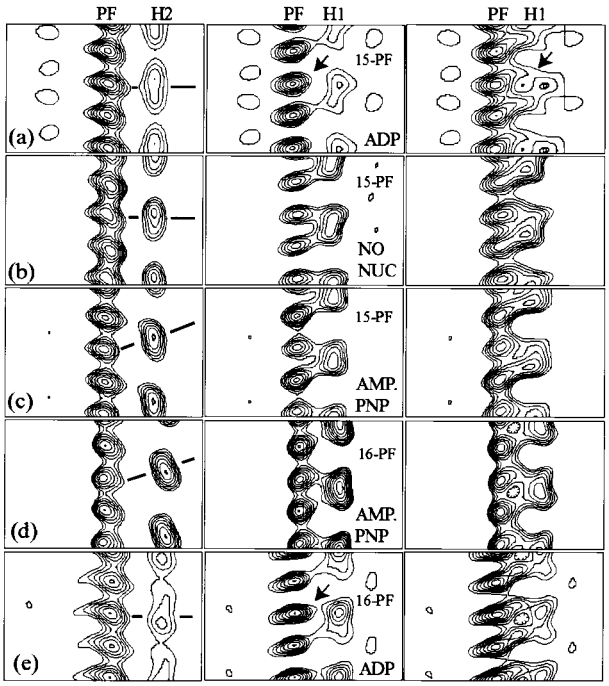

Figure 7. Sections through the five maps shown in Figure 6, cut through the microtubule axis at three different angles: the sections on the left pass through the middle of a tubulin protofilament (PF) and through the second (tethered) ncd heads (H2); the other two sections through each map differ in angle by only 2.4 degrees and show adjacent regions of the directly attached heads (H1). The order of the maps is the same as in Figure 6. Sloping lines in the left-hand sections indicate the positions of the tethered heads relative to the subunits of the microtubule; in AMP.PNP (c) and (d), the tethered heads are shifted more towards the microtubule plus end (top of page). The presence of ADP (a) and (e) reduces the apparent density of both heads, compared with those in (b) to (d), and makes the attached heads appear more weakly associated with tubulin (see middle sections, especially).

expressed in the maps (Figures 5, 7 and 8) is also significant.

Interestingly, the heads in Figure 8(a) are weaker than those in 8(c), even though the two maps were calculated using identical amplitudes. Clearly, phase changes on the (15,0) and other layerlines cause the density associated with ncd to be spread over a wider volume in the map of the ADP state; this result provides direct evidence for a greater disorder of heads bound in the ADP-filled state and it is not necessary to suppose that the low density of the heads in the original maps and the associated weakness of the 8-nm layerline are due only to partial decoration.

Discussion

Dimeric ncd attaches to microtubules by only one of its two heads under all three nucleotide conditions. In the two strongly bound states, the directly attached head makes contact with a pair of tubulin subunits. This is consistent with findings by cross-linking (Walker, 1995) and blot overlay (Larcher *et al.*, 1996) that both kinesin and ncd can be cross-linked to α and β-tubulin. Previously published maps of microtubules or tubulin sheets decorated with kinesin or ncd in AMP.PNP have shown an attached kinesin or ncd head situated over the boundary between the two subunits of a tubulin heterodimer (reviewed by Amos & Hirose, 1997) and, in most maps it appears to make contact

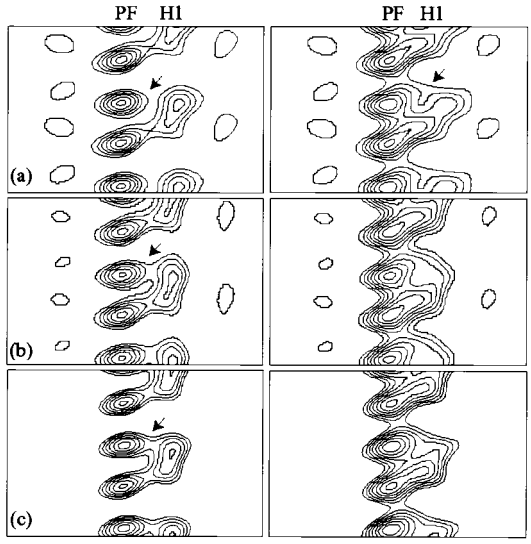

Figure 8. Sections through hybrid maps, cut at the same angles as the central and right-hand sections of Figure 7. All three maps were calculated using layerline amplitudes obtained by averaging the ADP and no nucleotide datasets for 15-pf microtubules (i.e. (a) and (b) of Figure 7). (a) and (c) of the present Figure were obtained using all the original phases from the ADP dataset (a) or all those from the no-nucleotide datasets (c); (b) was calculated using the same data as for (a), except that phases on the (15,0) layerline came from the no-nucleotide dataset. Subtle differences in the way that ncd heads appear to attach to tubulin are thus correlated with the phase changes on the (15,0) layerline.

with both subunits. However, there have been some variations in detail. After re-orienting each map so that the microtubule plus ends point upwards, the map of Kikkawa *et al*. (1995), of kinesin strongly attached to 10-pf microtubules, those of Sosa & Milligan (1996), of ncd strongly attached to 15-pf microtubules and those of Hoenger *et al*. (1995) and Hoenger & Milligan (1997), of ncd and kinesin strongly attached to tubulin sheets, have a slightly denser interaction with the β-tubulin monomer, nearer the plus end. Our new map of ncd bound to 15-pf microtubules in the presence of AMP.PNP (Figure 7(c)) also shows the motor attached to a pair of monomers, though with a slightly denser connection to the α-tubulin monomer.

In contrast, maps calculated by Arnal *et al*. (1996) show both kinesin and ncd attached only to the monomer nearer the minus end. The reason for this difference is unclear but could be related to the level of underfocus, which can have a significant effect on subtle features such as the way that strong features appear to be connected. The greater depth of underfocus used to record the images of Arnal *et al*. (1996) (2000 to 3000 nm) puts more emphasis on lower resolution features such as the protofilament striations; it also explains why the tubulin subunits and motor domains all appear longer and thinner than in other maps. The smaller variations among the maps produced by other laboratories could perhaps be due to smaller differences in underfocus levels or even to different contrast transfer functions imposed on the data during densitometry of the micrographs.

The new maps presented here are from consistent sets of data; specimens were prepared in equivalent ways, imaged at the same level of underfocus, the images were all densitometered equivalently and the digitised data treated consistently, so differences in the maps should represent real differences in the specimens. Dimeric ncd molecules attach to the microtubules by one head under all the conditions studied here, while the free head appears to be tethered in a relatively fixed position, as shown previously for the AMP.PNP state (Hirose *et al*., 1996; Arnal *et al*., 1996). Details of the interaction with the microtubule are similar in the presence of AMP.PNP and in the absence of nucleotide, the attached head apparently making close contact with both subunits of a tubulin heterodimer, but the ADP state shows a significant reduction in density where the motor interacts with beta tubulin. The apparent loosening in the motor-tubulin interaction seen by electron microscopy fits in well with the weaker binding measured in solution (Crevell *et al*., 1996).

The crystal structure of ncd complexed with ADP (Sablin *et al*., 1996) has been fitted into density representing attached ncd heads attached to microtubules in the presence of AMP.PNP, in maps obtained by electron microscopy (Sosa *et al*., 1997; Hirose & Amos, 1998). The structural changes we now observe to result from differences in bound nucleotide mean that the fitting process can only have been approximately correct. Also, there appear to be local conformational changes in and near the loops when the motors make contact with tubulin, as indicated by spin-labelling of Cys670; this residue, which lies close to loop L12 in the ncd motor domain, shows a big change in mobility when the motor is bound to microtubules (Naber *et al*., 1997). Nevertheless, the regions of the motor surfaces predicted to contact tubulin are in good agreement with other evidence: this includes whole-segment mutagenesis studies showing that residues 1 to 130 of kinesin, on the other side of the molecule, are not needed for microtubule binding (Yang *et al*., 1989); mutagenesis of individual residues correlated with microtubule-stimulated ATPase and motility assays (Woehlke *et al*., 1997); and results obtained by proteolytic mapping of kinesin and ncd (Alonso *et al*., 1998).

Both motors probably make contact with tubulin *via* loops L11 and L12, which form a band across the centre of the head and possibly also *via* loop L8 at the top of the head. At the base of the ncd head, a loop (L2) that is almost absent from the kinesin structure is likely to make an additional contact. The present results suggest that ADP-binding to ncd may weaken the possible contact between tubulin and L8. There is no evidence from the

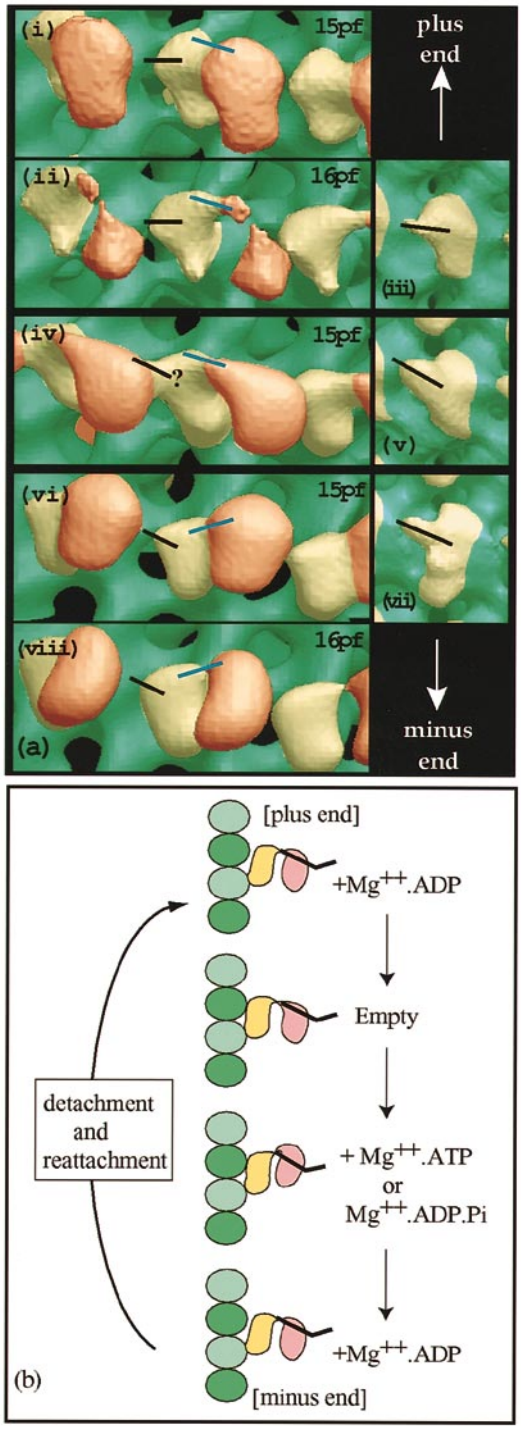

Figure 9. (a) Surface representations of all five maps of microtubules complexed with dimeric ncd and imaged in ice (i, ii, iv, vi, viii), compared with results obtained with negative stain (Hirose *et al*., 1995) for single-headed kinesin (KΔ340) complexed with cricket microtubules (iii, v, vii). The attached heads (yellow) of kinesin or ncd show similar features for specimens in ice and negative stain; the two motors also appear to undergo similar conformational changes as their nucleotide content varies; black bars indicate the angle of a protruding feature (the spike). (i) to (iii) With ADP, (iv) to (v) with no nucleotide, (vi) to (viii) with AMP.PNP. Blue bars indicate the angle at which the tethered heads (orange) appear to be connected to the attached heads. The tethered heads in (ii) appear poorly connected because the small number of 16-pf brain microtubules available for averaging did not allow the noise to be reduced adequately. (b) Diagram showing the simplest possible series of conformational changes consistent with our results, as an attached ncd motor domain goes through a cycle of Mg^{2+}.ATP hydrolysis. The ADP-containing state that we observe in the complexes could be equivalent to one that occurs when a head first attaches (top) and is about to lose its bound Mg^{2+}.ADP or to the state (bottom) after the hydrolysis of ATP and release of the γ-phosphate (Pi). Microtubules were decorated in the absence of added nucleotide, before the addition of ADP, and may have been driven backwards into the initial state. We see two independent structural changes, involving the motor-microtubule interaction and the motor-motor connection, respectively. The change that allows the motor to interact strongly with tubulin (two middle stages) occurs if Mg^{2+}.ADP is either absent or balanced by Pi, whereas tilting of the tethered head towards the plus-end occurs only when Pi is present.

images of ADP-kinesin, in negative stain (Hirose *et al*., 1995), for an ADP-induced loosening of the contact between tubulin and the top of the kinesin head but this point needs to be checked by cryoelectron microscopy of kinesin in the presence of different nucleotides.

Our evidence for a nucleotide-dependent change in the shape of the motor domains agrees with the results of Alonso *et al*. (1998), showing that both motors have additional cleavage sites in the presence of ADP compared with those in AMP.PNP, whether or not the motors are associated with microtubules. There is a change in the observed shape of the attached ncd head, similar to that seen for kinesin heads in negative stain (Hirose *et al*., 1995; see Figure 9(a)) A protruding part of the monomeric kinesin under study (termed the ''spike'' in the previous work) appeared to tilt towards the microtubule plus end in the transition from the ADP-containing to the nucleotide-free state. We originally speculated that this protrusion might represent the connection to the tail of a kinesin dimer and that the change might facilitate movement towards the microtubule plus end. However, images of dimeric kinesin molecules subsequently (Arnal *et al*., 1996; Hirose *et al*., 1996) suggested that the tail connection was quite far away from this point. Now that ncd heads appear to show a similar movement in the same direction, it seems unlikely that motion of the spike relates directly to a ''power stroke'' type of conformational change: if it did, then the power stroke would be in the unproductive direction for ncd.

After a kinesin or ncd motor domain loses ADP, it binds a fresh molecule of ATP, if available, and hydrolyses it (e.g. Ma & Taylor, 1997). The conformation of ncd in the presence of AMP.PNP may be representative of motors occupied by ATP or by ADP.Pi. Compared with the nucleotide-free and ADP states, the angle of the tethered head in the AMP.PNP state is changed, reaching more towards

the plus end. If the AMP.PNP state is fairly representative of the ATP state, our results would suggest that when ATP binds to the attached ncd head, it actually moves the tethered head in the wrong direction, away from the next appropriate target. As illustrated in Figure 9(b), this ''reverse stroke'' could be cancelled out by an equal movement towards the minus end, during the transition to the ADP-filled state. Alternatively, there may be a structural difference between ADP-containing heads attached to microtubules at the two distinct stages in the ATPase cycle. Some form of hysteresis in the conformational state of kinesin or ncd motor domains may explain the ability of single heads to progress along microtubules. In this case, the oppositely directed movements of monomeric kinesin and ncd might be due to attachment by different loops at different stages, especially during the weakly bound states (Lockhart & Cross, 1994).

With regard to the extent of interaction between the two heads of an ncd dimer, reconstructed images of microtubules decorated in the presence of AMP.PNP have shown some variation. In some images (Arnal *et al*., 1996; Hirose *et al*., 1996) the heads are definitely joined only near the top of the bound head, assumed to be where the coiled-coil tail is connected, but there is another possible contact where the lower tips of both heads curve towards each other. This pair of contacts at the upper and lower tips of the heads seem to have merged to give the appearance of a continuous line of close interaction in other images (Sosa & Milligan, 1996; Figure 5(c) of the present work). In the presence of ADP or absence of nucleotide, on the other hand, there is clearly only one region of contact between a pair of heads; it does, however, seem to be more extensive than a single point resulting from the association of the unseen coiled-coil segment. It is likely that some form of communication between the two heads of a dimer allows them to function in a coordinated manner.

The structure of double-headed kinesin has been studied only in the presence of AMP.PNP (Hirose *et al*., 1996; Arnal *et al*., 1996). Compared to the position of the unattached head of kinesin, the unattached head of ncd is closer to the minus end in all three states studied here. The relative arrangement of the heads of the ncd dimers should bias movement of the tethered head towards a new attachment site closer to the microtubule minus end. As discussed elsewhere (Cross, 1997), directional movement of dimeric motors probably results from a combination of the intrinsic properties of the individual motor domains and the relative arrangement of the two heads. The results presented here support a model involving directionally biased diffusion of the motor domains (e.g. Huxley, 1957; Vale & Oosawa, 1990; Cordova *et al*., 1992; Leibler & Huse, 1993) and re-inforce the idea that the relationship between the head and stalk domains is important in determining the direction of movement (Case *et al*., 1997; Henningsen & Schliwa, 1997).

Materials and Methods

Microtubules were assembled from purified pig brain tubulin in a polymerising solution (80 mM Pipes (pH 6.8), 1 mM EGTA, 5 mM $MgCl_2$, 1 mM DTT, 1 mM GTP, 5% (v/v) DMSO), stabilised with taxol, centrifuged, and resuspended in a solution without GTP. DMSO was added in order to increase the proportion of 15-pf microtubules (Ray *et al*., 1993). NΔ295-700 was expressed and purified as described (Lockhart *et al*., 1995). Microtubules diluted in the Mes solution (20 mM Mes, 2 mM $MgSO_4$, 1 mM EGTA, 1 mM DTT, 10 μM taxol, pH 6.5) were applied to an EM grid coated with a holey carbon film, and NΔ295-700 were then added to be 10 μM. Motility of NΔ295-700 in this solution was checked by a microtubule gliding assay. For freezing in the AMP.PNP and no nucleotide states, the microtubule-ncd mixture was incubated on the grid with 1 mM AMP.PNP and 2 units/ml apyrase, respectively, and then rapidly frozen by plunging them into an ethane slush. For the ADP state, the microtubule-ncd mixture was put on to the grid first and 1 mM ADP, 1 unit/ml hexokinase, and 0.01% (w/v) glucose were added just before freezing. The grids were examined using a Gatan cold stage in a Philips EM 420 electron microscope operating at 120 kV and with a defocus of 1300 to 1600 nm. Images were photographed at a magnification of 36,000×. The micrographs were scanned using a Zeiss Phodis scanner in 28μm steps.

Images of microtubules with 15 or more protofilaments were selected initially by measuring their diameters and then by inspecting their Fourier transform patterns (Figure 2). If the layerline intensities of the computed transforms had mirror symmetry, their phases were tested for consistency with helical symmetry of 15-pf or 16-pf microtubules. Transform data from different images were then compared; the phases in each dataset were adjusted to match, as well as possible, those of a reference image, by altering the axial position of the phase origin and allowing for a difference in the rotation about the axis. The final average included only images for which both sides were completely consistent with the consensus, in order to be sure of avoiding microtubules with ''seams'' in the helical lattice (Song & Mandelkow, 1995; Sosa & Milligan, 1996; Metoz *et al*., 1997).

In order to be able to compare complexes under different conditions, micrographs were recorded with a consistent exposure and the images were scanned in the same manner. The digitised images were boxed and floated consistently before their Fourier transforms were calculated. No subsequent adjustments were made to the relative scales of different datasets. Averaging was carried out using reciprocal space data. Maps calculated from these data were displayed as previously (Hirose *et al*., 1995, 1996).

Acknowledgements

We are very grateful to Juan Fan for providing purified tubulin and to Andrew Lockhart and Maria Alonso for purified ncd protein.

References

Alonso, M. C., van Damme, J., Vanderkerckhove, J. & Cross, R. A. (1998). Proteolytic mapping of kinesin/ncd-microtubule interface: nucleotide-dependent

conformational changes in the loops L8 and L12. *EMBO J.* **17**, 945–951.
Amos, L. A. & Cross, R. A. (1997). Structure and dynamics of molecular motors. *Curr. Opin. Struct. Biol.* **9**, 4–11.
Amos, L. A. & Hirose, K. (1997). The structure of microtubule-motor complexes. *Curr. Opin. Cell Biol.* **7**, 239–246.
Arnal, I., Metoz, F., DeBonis, S. & Wade, R. H. (1996). Three-dimensional structure of functional motor proteins on microtubules. *Curr. Biol.* **6**, 1265–1270.
Case, R. B., Pierce, D. W., Hom-Booher, N., Hart, C. L. & Vale, R. D. (1997). The directional preference of kinesin motors is specified by an element outside of the motor catalytic domain. *Cell,* **90**, 959–966.
Chandra, R., Salmon, E. D., Erickson, H. P., Lockhart, A. & Endow, S. A. (1993). Structural and functional domains of the *Drosophila* ncd microtubule motor protein. *J. Biol. Chem.* **268**, 9005–9013.
Cordova, N. J., Ermentrout, B. & Oster, G. F. (1992). Dynamics of single-motor molecules: the thermal ratchet model. *Proc. Natl Acad. Sci. USA,* **89**, 339–343.
Crevel, I. M.-T. C., Lockhart, A. & Cross, R. A. (1996). Weak and strong states of kinesin and ncd. *J. Mol. Biol.* **257**, 66–76.
Crevel, I. M.-T. C., Lockhart, A. & Cross, R. A. (1997). Kinetic evidence for low chemical processivity in ncd and Eg5. *J. Mol. Biol.* **273**, 160–170.
Cross, R. A. (1997). Reversing the kinesin ratchet: a diverting tail. *Nature,* **389**, 15–16.
de Cuevas, M., Tao, T. & Goldstein, L. S. (1992). Evidence that the stalk of *Drosophila* kinesin heavy chain is an alpha-helical coiled coil. *J. Cell Biol.* **116 (4)**, 957–965.
Gelles, J., Berliner, E., Young, E. C., Mahtani, H. K., Perezramirez, B. & Anderson, K. (1995). Structural and functional features of one-headed and two-headed biotinated kinesin derivatives. *Biophys. J.* **68**, 276s–282s.
Hackney, D. D. (1994). Evidence for alternating head catalysis by kinesin during microtubule-stimulated ATP hydrolysis. *Proc. Natl Acad. Sci. USA,* **91**, 6865–6869.
Henningsen, U. & Schliwa, M. (1997). Reversal of the direction of movement of a molecular motor. *Nature,* **389**, 93–96.
Hirose, K. & Amos, L. A. (1998). Three-dimensional structure of motor molecules. *Cell. Mol. Life Sci.* In the press.
Hirose, K., Lockhart, A., Cross, R. A. & Amos, L. A. (1995). Nucleotide-dependent angular change in kinesin motor domain bound to tubulin. *Nature,* **376**, 277–279.
Hirose, K., Lockhart, A., Cross, R. A. & Amos, L. A. (1996). Three-dimensional cryoelectron microscopy of dimeric kinesin and ncd motor domains on microtubules. *Proc. Natl Acad. Sci. USA,* **93**, 9539–9544.
Hirose, K., Amos, W. B., Lockhart, A., Cross, R. A. & Amos, L. A. (1997). Three-dimensional cryoelectron microscopy of 16-protofilament microtubules: structure, polarity and interaction with motor protein. *J. Struct. Biol.* **118**, 140–148.
Hoenger, A. & Milligan, R. A. (1997). Motor domains of kinesin and ncd interact with microtubule protofilaments with the same binding geometry. *J. Mol. Biol.* **265**, 553–564.
Hoenger, A., Sablin, E. P., Vale, R. D., Fletterick, R. J. & Milligan, R. A. (1995). 3-Dimensional structure of a tubulin-motor-protein complex. *Nature,* **376**, 271–274.
Huang, T. G., Suhan, J. & Hackney, D. D. (1994). *Drosophila* kinesin motor domain extending to amino-acid position-392 is dimeric when expressed in *Escherichia-coli*. *J. Biol. Chem.* **269**, 16502–16507.
Huxley, A. F. (1957). Muscle structure and theories of contraction. *Prog. Biophys. Biophys.* **7**, 255–318.
Jiang, W. & Hackney, D. D. (1997). Monomeric kinesin head domains hydrolyze multiple ATP molecules before release from a microtubule. *J. Biol. Chem.* **272 (9)**, 5616–5621.
Jiang, W., Stock, M. F., Li, X. & Hackney, D. D. (1997). Influence of the kinesin neck domain on dimerization and ATPase kinetics. *J. Biol. Chem.* **272**, 7626–7632.
Kikkawa, M., Ishikawa, T., Wakabayashi, T. & Hirokawa, N. (1995). 3-Dimensional structure of the kinesin head-microtubule complex. *Nature,* **376**, 274–279.
Larcher, J. C., Boucher, D., Lazereg, S., Gros, F. & Denoulet, P. (1996). Interaction of kinesin motor domains with alpha- and beta-tubulin subunits at a tau-independent binding site: regulation by polyglutamylation. *J. Biol. Chem.* **271**, 22117–22124.
Leibler, S. & Huse, D. A. (1993). Porters versus rowers: a unified stochastic model of motor proteins. *J. Cell Biol.* **121**, 1357–1368.
Lockhart, A. & Cross, R. A. (1994). Origins of reversed directionality in the ncd molecular motor. *EMBO J.* **13**, 751–757.
Lockhart, A., Cross, R. A. & McKillop, D. F. A. (1995). ADP release is the rate-limiting step of the MT activated ATPase of non-claret disjunctional and kinesin. *FEBS Letters,* **368**, 531–535.
Ma, Y. Z. & Taylor, E. W. (1997). Interacting head mechanism of microtubule-kinesin ATPase. *J. Biol. Chem.* **272**, 724–730.
Macdonald, H. B., Stewart, R. J. & Goldstein, L. S. B. (1990). The kinesin-like ncd protein of *Drosophila* is a minus end-directed microtubule motor. *Cell,* **63**, 1159–1165.
Metoz, F., Arnal, I. & Wade, R. H. (1997). Tomography without tilt: three-dimensional images of microtubule/motor complexes. *J. Struct. Biol.* **118**, 159–168.
Morii, H., Takenawa, T., Arisaka, F. & Shimizu, T. (1997). Identification of kinesin neck region as a stable α-helical coiled coil and its thermodynamic characterization. *Biochemistry,* **36**, 1933–1942.
Moyer, M. L., Gilbert, S. P. & Johnson, K. A. (1996). Purification and characterization of two monomeric kinesin constructs. *Biochemistry,* **35**, 6321–6329.
Naber, N., Cooke, R. & Pate, E. (1997). Binding of ncd to microtubules induces a conformational change near the junction of the motor domain with the neck. *Biochemistry,* **36**, 9681–9689.
Ray, S., Meyhöfer, E., Milligan, R. A. & Howard, J. (1993). Kinesin follows the microtubule's protofilament axis. *J. Cell Biol.* **121**, 1083–1093.
Sablin, E. P., Kull, F. J., Cooke, R., Vale, R. D. & Fletterick, R. J. (1996). Crystal structure of the motor domain of the kinesin-related motor ncd. *Nature,* **380**, 555–559.
Sawin, K. E. & Endow, S. A. (1993). Meiosis, mitosis and microtubule motors. *BioEssays,* **15**, 399–407.

Song, Y. H. & Mandelkow, E. (1994). Paracrystalline structure of the stalk domain of the microtubule motor protein kinesin. *J. Struct. Biol.* **112**, 93–102.

Song, Y.-H. & Mandelkow, E. (1995). The anatomy of flagellar microtubules: polarity, seam, junctions, and lattice. *J. Cell Biol.* **128**, 81–94.

Sosa, H. & Milligan, R. A. (1996). Three-dimensional structure of ncd-decorated microtubules obtained by a back-projection method. *J. Mol. Biol.* **260**, 743–755.

Sosa, H., Dias, D. P., Hoenger, A., Whittaker, M., Wilson-Kubalek, E., Sablin, E., Fletterick, R. J., Vale, R. D. & Milliagn, R. A. (1997). A model for the microtubule-ncd motor protein complex obtained by cryo-electron microscopy and image analysis. *Cell,* **90**, 217–224.

Stewart, R. J., Thaler, J. P. & Goldstein, L. S. B. (1993). Direction of microtubule movement is an intrinsic property of the motor domains of kinesin heavy chain and *Drosophila* ncd protein. *Proc. Natl Acad. Sci. USA,* **90**, 5209–5213.

Tripet, B., Vale, R. D. & Hodges, R. S. (1997). Demonstration of coiled-coil interactions within the kinesin neck region using synthetic peptides. *J. Biol. Chem.* **272**, 8946–8956.

Vale, R. D. & Oosawa, F. (1990). Protein motors and Maxwell's demons: does mechanochemical transduction involve a thermal ratchet? *Advan. Biophys.* **26**, 97–134.

Vale, R. D., Reese, T. S. & Sheetz, M. P. (1985). Identification of a novel force-generating protein, kinesin, involved in microtubule-based motility. *Cell,* **42**, 39–50.

Walker, R. A. (1995). Ncd and kinesin motor domains interact with both alpha-tubulin and beta-tubulin. *Proc. Natl Acad. Sci. USA,* **92**, 5960–5964.

Walker, R. A., Salmon, E. D. & Endow, S. A. (1990). The *Drosophila* claret segregation protein is a minus-end directed motor molecule. *Nature,* **347**, 780–782.

Woehlke, G., Ruby, A. K., Hart, C. L., Ly, B., Hom-Booher, N. & Vale, R. D. (1997). Microtubule interaction site of the kinesin motor. *Cell,* **90**, 207–216.

Yang, J. T., Laymon, R. A. & Goldstein, L. S. B. (1989). A three-domain structure of kinesin heavy chain revealed by DNA sequence and microtubule binding analyses. *Cell,* **56**, 879–889.

Edited by R. Huber

(Received 17 November 1997; received in revised form 5 February 1998; accepted 12 February 1998)

Note added in proof: Images published by Arnal & Wade (1998) show double-headed kinesin in the presence of ADP and in the absence of nucleotide. Although the lateral position of the tethered kinesin head varies, it is always closer to the microtubule plus end. (Arnal, I. & Wade, R. H. (1998). *Structure*, **6**, 33–38.)